Article:

Betts, J.W., Roth, P., Pattrick, C.A. et al. (4 more authors) (2020) Antibacterial activity of Mn(i) and Re(i) tricarbonyl complexes conjugated to a bile acid carrier molecule. Metallomics, 12 (10). pp. 1563-1575. ISSN 1756-5901

https://doi.org/10.1039/d0mt00142b

Antibacterial activity of Mn(I) and Re(I) tricarbonyl complexes conjugated to a bile acid carrier molecule

Jono W. Betts,[a] Patrick Roth,[b] Calum A. Pattrick,[c] Hannah Southam,[c] Roberto La Ragione,[a] Robert K. Poole,[c] and Ulrich Schatzschneider[b*]

[a] *Department of Pathology and Infectious Diseases, School of Veterinary Medicine, University of Surrey, Guildford, United Kingdom*

[b] *Institut für Anorganische Chemie, Julius-Maximilians-Universität Würzburg, Am Hubland, D-97074 Würzburg, Germany*

[c] *Department of Molecular Biology and Biotechnology, The University of Sheffield, United Kingdom*

* Corresponding author: eMail: ulrich.schatzschneider@uni-wuerzburg.de;
Tel: +49 931 31 83636; Fax: +49 931 31 84605.

Abstract

A bifunctional cholic acid-bis(2-pyridylmethyl)amine (bpa) ligand featuring an amide linker was coordinated to a manganese(I) or rhenium(I) tricarbonyl moiety to give $[M(bpa^{cholamide})(CO)_3]$ with M = Mn, Re in good yield and very high purity. Strong antibacterial activity was observed against four strains of methicillin-susceptible (MSSA) and methicillin-resistant (MRSA) *Staphylococcus aureus*, with minimum inhibitory concentrations (MICs) in the range of 2–3.5 μM. No difference in response was observed for the MSSA *vs*. MRSA strains. Activity was also independent of the nature of the metal center, as the Mn and Re complexes showed essentially identical MIC values. In contrast to some other metal carbonyl complexes, the activity seems to be unrelated to the release of carbon monoxide, as photoactivation of the Mn complex reduced the potency by a factor of 2–8. Both metal complexes were non-toxic in *Galleria mellonella* larvae at concentrations of up to 100× the MIC value. *In vivo* testing of *Galleria* larvae infected with MRSA/MSSA demonstrated a significant increase in overall survival rates from 46% in the control to 88% in the group treated with the metal complexes. ICP-MS analysis showed that the Mn and Re cholamide complexes are efficiently internalized by *E. coli* cells and do not interfere with membrane integrity, as evident from a lack of release of intracellular ATP. An increased sensitivity was observed in *acrB*, *acrD*, *and mdt* mutants that are defective in multidrug exporters, indicating that the compounds have an intracellular mechanism of action. Furthermore, *E. coli mntP* mutants, defective in the gene encoding an Mn exporter, were more sensitive than the wildtype, while inactivation of the regulator that controls expression of the Mn uptake proteins MntP and MntH slightly increased sensitivity to the compound. Single knockout mutants defective in genes linked to bile salt and oxidative stress response (*dinF*, *yiaH*, *sodA*, *katE*, and *soxS*) did not show increased sensitivity relative to the wild type. Overall, neither the cholic acid moiety nor the metal-carbonyl fragment alone appear to be responsible for the biological activity observed and thus the search for the primary intracellular target continues.

Introduction

For many decades, bacterial infections were well-controlled by antimicrobial drugs based on a wide range of structural motifs. However, inappropriate and overuse together with the slow appearance of new antibiotics on the market due to a lack of development activity by the pharmaceutical industry have led to the emergence of an antimicrobial resistance (AMR) crisis,[1-3] as more and more bacterial strains become non-responsive to standard drugs and sometimes even drugs of last resort. In this serious situation, no part of the chemical space should be left unexplored for potential new drug candidates with novel mechanisms of action that cannot be evaded by bacterial resistance processes. In that context, (organo)metal compounds are a promsing source for new antibacterial drugs[4, 5] and contrary to common believe, can be subject to standard drug development procedures and optimization of ADMET properties.

Some recent large-scale nonbiased screening efforts have revealed a surprisingly high hit rate for metal-based antibacterial agents (approx. 10% of more than 900 compounds tested), which was even higher than that for purely organic compounds submitted to the same assays. Minimum inhibitory concentrations (MICs) down to the nanomolar range were observed on methicillin-resistant *Staphylococcus aureus* (MRSA).[5] Many of the tested compounds feature very elaborate co-ligands on the metal center and some are coordinated to established drugs, such as azole antimicrobials.[6] Conversely, much less is known about the antibacterial activity of (organo)metal fragments conjugated to biological carrier molecules. Promising results have been obtained with the systematic optimization of metallocenes attached to antimicrobial peptides (AMPs), which lead to identification of conjugates with low micromolar MIC values (5–10 μM).[7] Still, there is very little work on other bio-derived carrier groups for metal-based antibacterial drug candidates.

Interestingly, for about two decades, cholic acid derivatives have been explored as potential mimics of squalamine and polymyxin B antibiotics (Chart 1),[8-10] although studies of the biological activity of cholane and norcholane derivatives date back to the 1950s.[11] As many of these compounds carry charged or at least highly polar functional groups,[12-14] we became interested in the functionalization of such cholic acid-related carrier molecules with cationic metal complex fragments.[15]

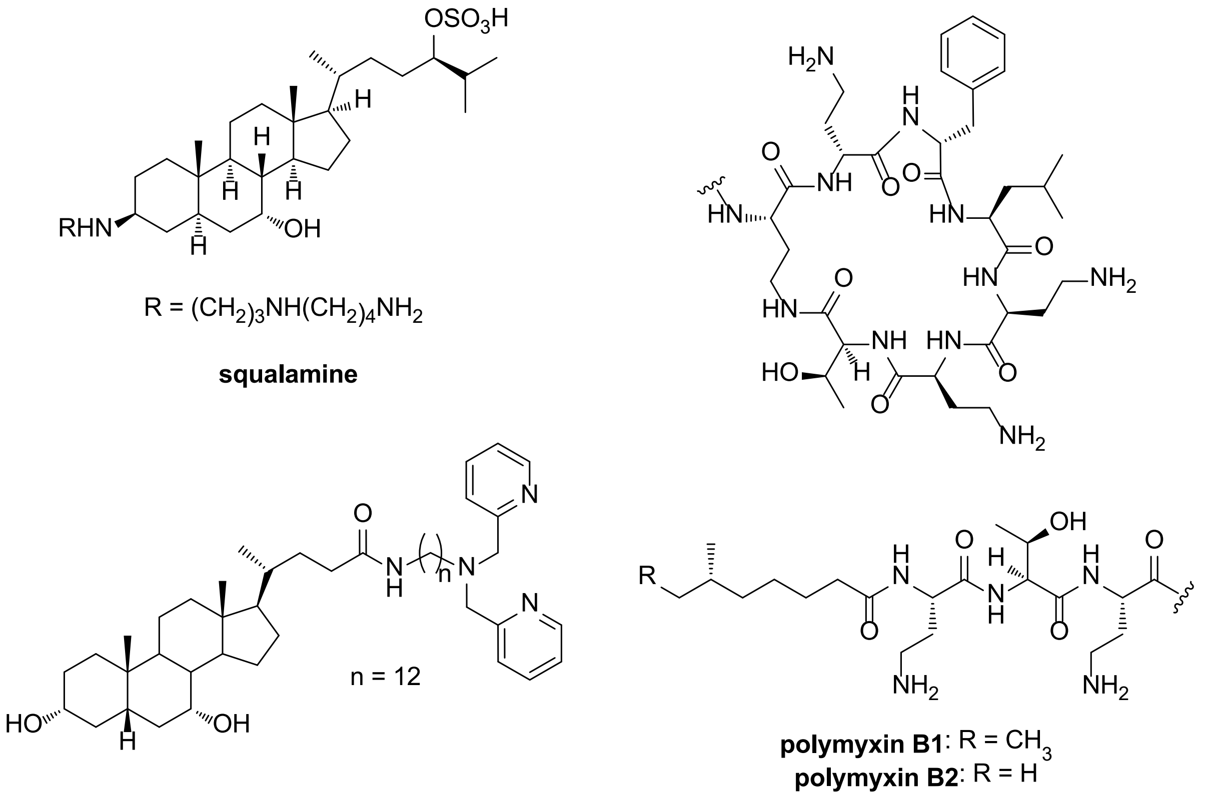

Chart 1. Structure of some cholic acid derivatives explored for antibiotic activity comparable to that of polymyxin B1 and B2.

A number of such compounds based on technetium(V) and gadolinium(III) have been evaluated for use as contrast agents in radioimaging[16, 17] and magnetic resonance imaging (MRI).[18] However, Shen and coworkers also reported on the antibacterial and antifungal activity of a bifunctional bile acid-bpa conjugate, although no metal complexes of this ligand were prepared.[19] Based on our own experience with tridentate bis(2-pyridiylmethyl)amine (bpa) ligands,[20, 21] which easily bind to a wide range of transition metals in either a square-planar or facial octahedral coordination mode, manganese(I) and rhenium(I) tricarbonyl complexes of such a bifunctional chelator-cholic acid conjugate appeared to be an interesting synthetic target.

Results and Discussion

Synthesis and characterization

For facile bioconjugation to the cholic acid carrier molecule, which is easily commercially available, a ligand with a pendant aminoalkyl linker was required as the coupling partner. Although we have also explored tris(pyrazolyl)methane (tpm)[22-25] and bis(pyrazolyl)-ethylamine (bpea)[26, 27] ligands in the past, based on the promising antibacterial activity of manganese tricarbonyl complexes with bis(2-pyridylmethyl)amine (bpa) chelators and their tetradentate tpa analogues,[20, 21, 28-30] a bpa ligand with a 2-aminoalkyl group as the "third arm" on the central tertiary amino group was selected. Although *N*,*N*-bis(2-pyridylmethyl)ethan-1,2-diamine (bpen) **4** is accessible by a variety of synthetic methods,[31-33] the compound turned out to be prone to decomposition in our hands and therefore, a direct route to a protected bpen derivative was explored, from which **4** was to be released and then directly used in the next step. In contast to Boc-protected 1,2-ethylenediamine (en) serving as a key building block, for example in the syntheses reported by Nagano[32] and Finney,[33] our approach is based on acetyl-protected bpen **3**, as this ligand could also serve as a non-targeted control. Therefore, 2-methyl-4,5-dihydro-1*H*-imidazole (lysidine) **2** was heated to 75 °C in water for 2 h to release *N*-acetyl-1,2-ethylenediamine.[34] Then, two equivalents of 2-(chloromethyl)pyridine hydrochloride **1** were added and slowly neutralized with an excess of 10 M sodium hydroxide. After further heating, extraction, and purification through a short alumina column, *N*-acetyl-protected bpen **3** was isolated in analytically pure form on close to a 10 g scale as a beige solid in decent yield and suitable for long-term storage (Scheme 1 top).[35] The acetyl protective group was removed by reflux in concentrated hydrochloric acid for 24 h and free bpen **4** obtained in near-quantitative yield as a pale yellow oil. Since the compound is prone to decomposition, it was directly conjugated to cholic acid **5** in tetrahydrofuran with *N*,*N'*-dicyclohexylcarbodiimide (DCC) and *N*-hydroxysuccinimide (NHS) as the coupling agents and *N*,*N*-diisopropylethylamine (DIPEA) as base (Scheme 1 center). After column chromatography on silica using a mixture of dichloromethane and methanol (5:1 v/v) as the eluent, the bifunctional cholic acid-bpa ligand **6** was obtained in good yield on a gram scale in analytically pure form. The successful coupling is evident in the ^{1}H and ^{13}C NMR spectrum of **6** from the amide group signal at 7.77 and 172.43 ppm, respectively. Furthermore, the two peaks of the ethylene linker also show notable shift differences between **4** and **6**. In particular, the triplet of the distal methylene group – the one adjacent to the amide nitrogen atom – moves from 2.63 ppm in **4** to 3.19 ppm in **6**, while the signal of the proximal methylene protons next to the bpa moiety only shifts by 0.04 ppm to lower field. The ^{13}C NMR spectrum is also indicative of the successful coupling, as the two ethylene linker peaks move from 57.23 and 39.40 ppm in **4** to 53.17 and 36.62 ppm in **6**, respectively, for the proximal and distal carbon atoms. Remarkably, in the 125 MHz ^{13}C NMR of conjugate **6**, all 32 independent signals for the cholic acid and bpa moieties as well as the linker could be clearly detected and assigned with the aid of HSQC and HMBC. Other literature procedures for the synthesis of **6** used the reductive amination of *N*-2-(aminoethyl)cholamide with 2-pyridine carboxaldehyde and sodium triacetoxyborohydride in higher overall yield,[13, 19] but we prefer the DCC/NHS-mediated coupling of **4** and **5** as shown in Scheme 1, as it also allowed conjugation of the bpa building block to other carboxylate-functionalized biological carrier molecules.

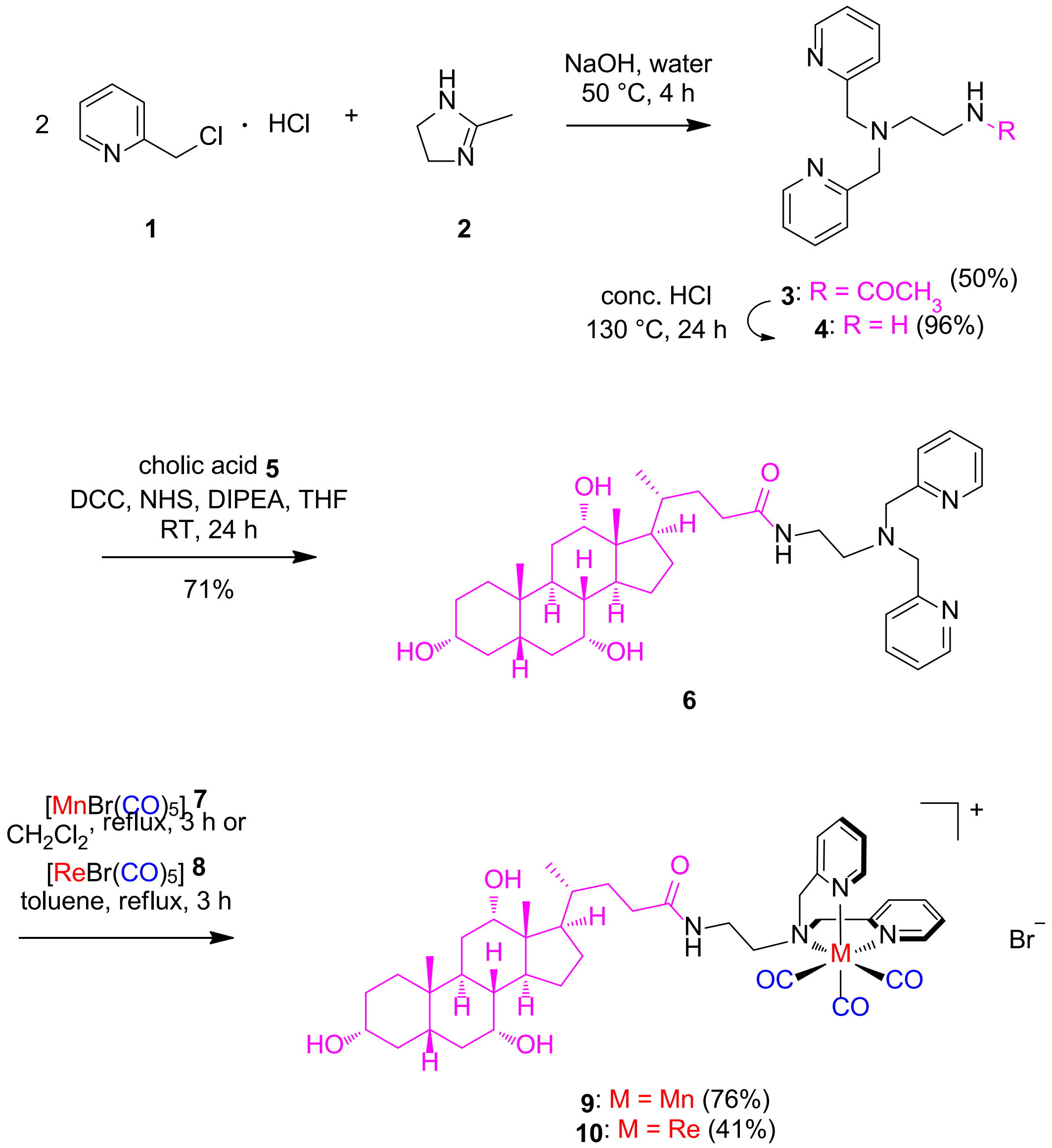

Scheme 1. Synthesis of metal tricarbonyl complexes **9** and **10** by reaction of cholic acid-conjugated bis(2-pyridylmethyl)amine (bpa) ligand **6** with manganese(I) or rhenium(I) pentacarbonyl bromide **7** or **8** at reflux in dichloromethane or toluene. The central amide coupling step uses *N*,*N*'-dicyclohexylcarbodiimide (DCC) and *N*-hydroxysuccinimide (NHS) as the activating agents and *N*,*N*-diisopropylethylamine (DIPEA) as base.

The metal tricarbonyl complexes were then easily prepared by reflux with metal pentacarbonyl bromides **7** or **8**. While the synthesis of manganese compound **9** was carried out in dichloromethane, the preparation of the rhenium analogue **10** required use of higher boiling toluene for successful preparation. In both cases, excess ligand and metal precursor were simply washed away with proper solvent to obtain Mn complex **9** as a yellow powder in 76% yield, while the Re congener **10** was isolated as a colorless solid in a somewhat lower yield of 41% (Scheme 1 bottom). In both cases, elemental analysis required the inclusion of some water of solvation, which is not surprising given the number of polar groups in the title compounds. ESI mass spectrometry showed the $[M\text{-}Br]^+$ species as the only notable peak in the whole measured range (see Fig. 1 and Supporting Information).

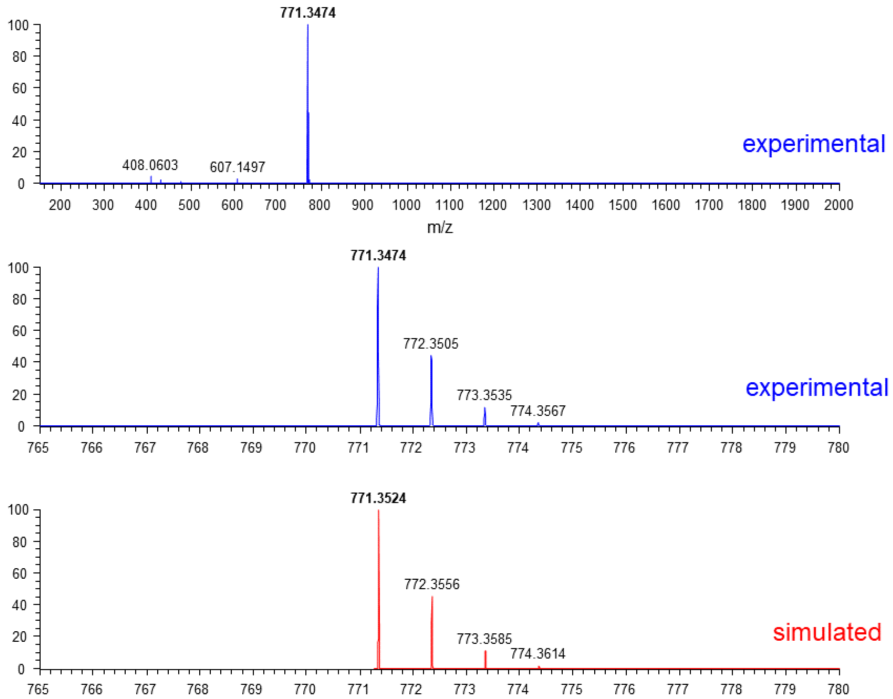

Figure 1. The ESI mass spectrum of manganese tricarbonyl complex **9** in methanol shows only the signal of the $[M\text{-}Br]^+$ species with an excellent match of the isotope pattern. The difference between experimental and calculated exact mass is -0.005 Da.

Most of the ^1H and ^{13}C NMR signal exhibit only very minor shifts upon metal coordination, but there are some notable differences in the peaks assigned to the bpa moiety, which are fortunately clearly distinct from the complicated and often overlapping cholic acid signals. Most diagnostic of metal coordination in bpa complexes is the splitting of the methylene group signal, which appears as a singlet with an intensity of 4H at 3.76 ppm in free ligand **4**, but gives rise to two geminal doublets at 4.88 and 4.71 ppm in **9** *vs*. 5.04 and 4.95 ppm in **10**, with ^2J coupling constants of 17 Hz. Some downfield shift is also evident for the pyridine H6 protons in proximity to the ring nitrogen atoms, which move from 8.46 ppm in **4** to 8.87 and 8.80 ppm in **9** and **10**, respectively. The methylene ^{13}C signals move from 59.59 ppm in the free ligand **4** to 66–67 ppm in metal complexes **9** and **10**. Interestingly, even the often very weak metal carbonyl signals were detected in the expected 2:1 ratio for the Mn compound at 218.90 and 218.35 ppm and for the Re complex at 196.38 and 195.16 ppm. The amide proton peak also experiences a notable downfield shift, as it appears as a triplet at 7.77 ppm in free ligand **4**, but moves to 8.10 ppm in **9** and **10**. As the ligand and metal complex ^{1}H NMR spectra were recorded in the same solvent (DMSO-d_6), this might be indicative of an interaction of the amide NH with the metal carbonyl groups.

Biological activity

Strong antibacterial activity for the two [M(bpen^{cholamide})$(CO)_3$]Br complexes **9** and **10** was observed against all four tested strains of methicillin-susceptible (MSSA) *vs*. methicillin-resistant (MRSA) *Staphylococcus aureus*, with minimum inhibitory concentrations (MICs) in the range of 2.3–3.1 µM for **9** (M = Mn) and 2–3.4 µM for **10** (M = Re), respectively (Table 1 top). No relevant differences in response were observed for the methicillin-susceptible *vs*. methicillin-resistant strains. Exchange of the metal center from Mn to Re also did not significantly influence the MIC values. The activity of both complexes is comparable to antibiotics currently licensed for *S. aureus,* such as amikacin, where wild type MIC distributions range between 1 and 30 µM. [The European Committee on Antimicrobial Susceptibility Testing. Breakpoint tables for interpretation of MICs and zone diameters. Version 10.0, 2020. http://www.eucast.org. -> That's another "grey" literature - we need "real" citations] In a recent study screening 906 metal complexes, including those of Mn, Cu, Ru and Ag, 246 compounds showed MICs equal or lower than 10 µM against one or more pathogens. However, MIC values reported for Mn complexes in that study were between 5 and 175 µM against *S. aureus*. Thus, complexes **9** and **10** have greater antibacterial activity than any of the Mn complexes reported.[5]

As metal carbonyl complexes have been widely explored as CO-releasing molecules (CORMs) with a potential light-triggered release of carbon monoxide,[36, 37] the effect of illumination on the biological activity was also studied. MIC values of the rhenium compound **10** were not affected at all by exposure to UV light (Table 1 center), in line with the general photostability of $Re(CO)_3$ complexes. In the case of the manganese complex **9**, differences between illuminated *vs*. non-illuminated samples were only observed for the highly responsive bacterial strains and photoactivation generally reduced the potency by a factor of 2–8, indicating that it is the intact metal tricarbonyl moiety which is relevant for the antibacterial activity. Some small deviations between the MSSA *vs*. MRSA and photoactivation MIC values are possibly due to sublte differences in the cell culture conditions, as these assays were carried out by different laboratories. [US: Previous sentence sufficient as an explanation?!? JB: We need to decide which values to proceed with here. I don't believe the addition of both our results is wise as our values are slightly different (mine are mean values). Although the data showing the comparison of +/- UV is very useful, all my further work (time-kills and Galleria assays) are based on my MICs. I also have MICs for strains of Streptococci, Acinetobacter, Pseudomonas and Enterococci] Other bacterial strains, including MG1655 as a common wildtype *E. coli* strain, EC958 as an example of uropathogenic *E. coli*, and AB184 and AB210 as clinically isolated multidrug-resistant *A. baumannii* strains, were also tested, but generally not very responsive towards both compounds (Table 1 bottom). The Re complex seems to be somewhat more active, but MIC values were high, with the most responsive AB184 showing a MIC of 32 μM.

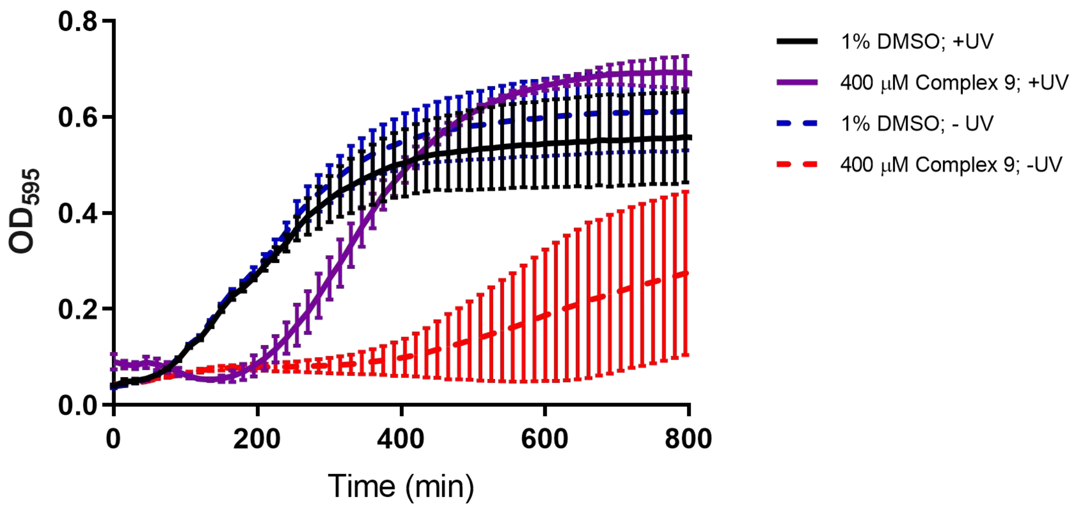

Figure 2. Antimicrobial effect of **9** (at a sub-MIC level) against wildtype BW25113 *E. coli*, with (purple line) and without (red line) UV light exposure at ___ nm for ___ min. Black and blue lines indicate treatment with 1% DMSO as a control with and without UV photoactivation, respectively. All data points are the mean of at least three biological replicates, with errors bars representing the standard deviation.

Table 1. Mean minimum inhibitory concentration (MIC) of [M(bpen^{cholamide})$(CO)_3$]Br **9** (M = Mn) and **10** (M = Re) *vs*. strains of methicillin-resistant *S. aureus* (MRSA) and methicillin-susceptible *S. aureus* (MSSA) as well as strains of *E. coli* (MG1655, EC958) and *A. baumannii* (AB184, AB210). UV +/- indicates illumination (or not) of samples at 365 nm for 6 min.

Strain	UV	Mean minimum inhibitory concentrations of [M(bpen^{cholamide})$(CO)_3$]Br (in µM)	
		9 (M = Mn)	**10** (M = Re)
MSSA NCTC 12981	-	3.1	3.4
MSSA SH1000	-	2.3	2.7
MRSA NCTC 12493	-	2.3	2.7
MRSA USA300	-	2.3	2.0
SH1000	-	4	4
	+	32	4
USA300	-	8	4
	+	16	4
MG1655	-	>1024	1024
	+	>1024	1024
EC958	-	>1024	256
	+	>1024	256
AB210	-	256	64
	+	256	64
AB184	-	64	32
	+	128	32

The effect of UV light exposure on bacterial cell growth as determined by optical density at 595 nm was also studied in a time-dependent manner in the presence and absence of Mn compound **9**. Illumination of 1% DMSO added to the cell culture, as required to solubilize the metal complexes, did not significantly affect bacterial growth (Fig. 2, dashed blue *vs*. solid black line). The addition of 400 µM of complex **9** with UV photoactivation led to some initial growth retardation, as the optical density remained low for the initial 200 min of the experiment, but then the bacteria started to grow and reached final OD levels comparable to the 1% DMSO controls (Fig. 2, solid violet line). The same concentration of metal complex in the absence of UV light resulted in a much longer inhibition of bacterial growth and final OD levels reached only about half of the maximum values observed for the other conditions, after 800 min of growth (Fig. 2, dashed red line).

Kill-kinetic assays indicate that Mn complex **9** is bactericidal against all four MRSA/MSSA strains tested, with >5 log lower bacterial numbers compared to the no drug control at 24 h and >2 log reduction in bacterial numbers when compared to the starting inocula (Fig. 3a-d). The rhenium analogue **10** showed bacteriostatic activity against three of the four strains (Fig. 3a, b and d). Although bacterial numbers initially reduce, after 24 h they recover to approximately that of the starting inocula. However, against MRSA NCTC 12493, complex **10** was bactericidal, with bacterial numbers reducing >3 log *vs*. the starting inoculum and >6 log reduction when compared to the no treatment control.

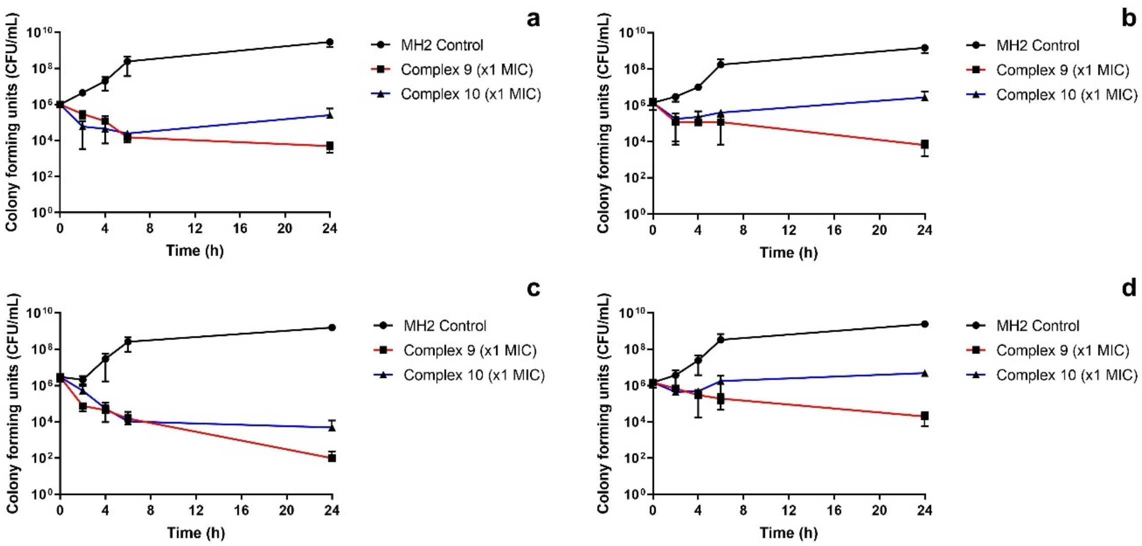

Figure 3. Kill-kinetics of [M(bpen^{cholamide})(CO)$_3$]Br **9** (M = Mn) and **10** (M = Re) against methicillin-susceptible *S. aureus* strains a) NCTC 12981, b) SH1000 and methicillin-resistant *S. aureus* strains c) NCTC 12493 and d) USA300; MH2 control: Mueller-Hinton 2 (MH2) cation-adjusted broth.

Both metal complexes **9** and **10** were non-toxic on *Galleria mellonella* at concentrations up to 100 times greater than those required for bacterial killing (Fig. 4). *In vivo* testing of larvae infected with MRSA/MSSA showed that treatment with [Mn(bpen^{cholamide})(CO)$_3$]Br **9** significantly increased survival compared to the PBS control ($p \leq 0.028$ for MSSA and $p \leq$

0.011 for MRSA), with overall survival rates of 88% (±7.98 percentage points [pp]) versus 46% (±10.95 pp) in the control group (Fig. 5).

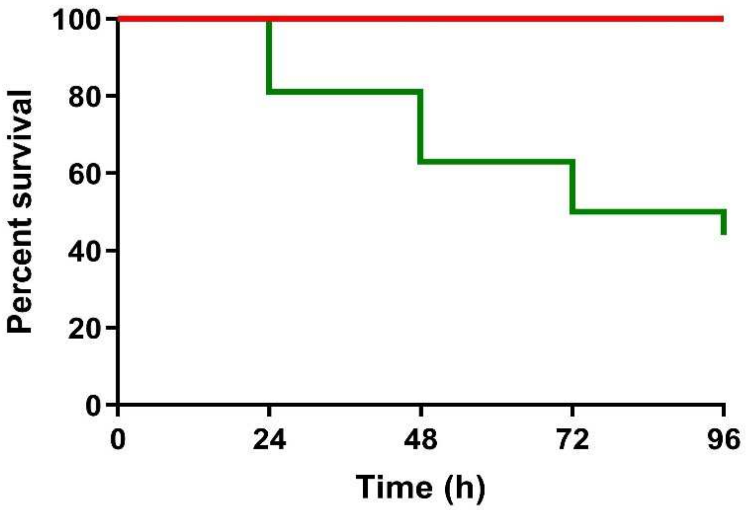

Figure 4. Precent survival of *G. mellonella* larvae upon exposure to [M(bpen^{cholamide})(CO)$_3$]Br **9** (M = Mn) at 100× MIC (red trace) compared to *S. aureus* NCTC 12981 (green trace). Treatment of the larvae with phosphate buffered saline (PBS), complex **9** at 10× MIC and complex **10** (M = Re) at 10× and 100× MIC gave survival curves identical to the red trace (data not shown for clarity).

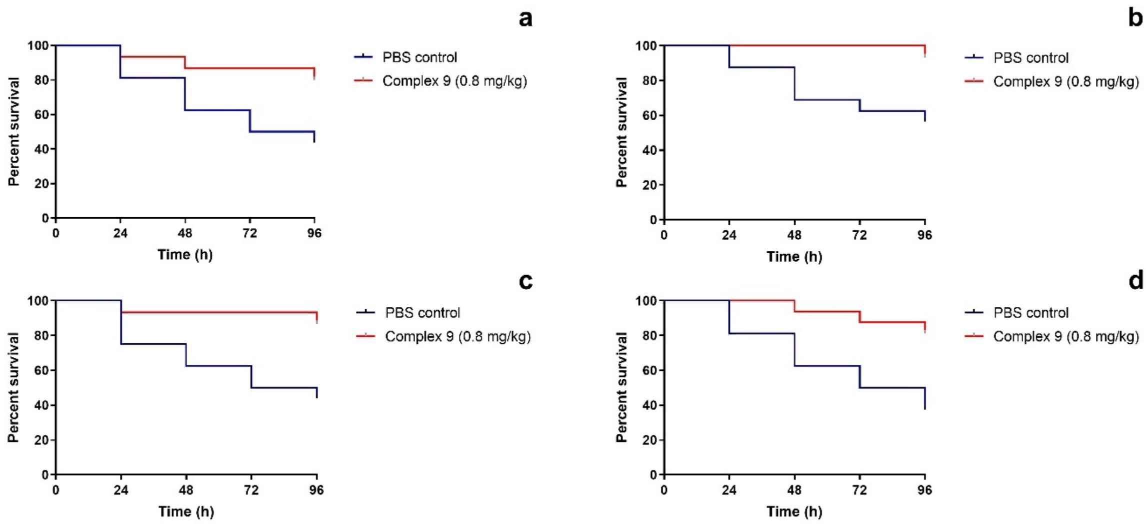

Figure 5. Survival curves for *G. mellonella* larvae infected with methicillin-susceptible *S. aureus* strains a) NCTC 12981, b) SH1000 and methicillin-resistant *S. aureus* strains c) NCTC 12493 and d) USA300 *via* left proleg injection, followed by right proleg injection of either PBS control or [Mn(bpen^{cholamide})(CO)$_3$]Br **9** dissolved in 5% DMSO at 0.8 mg/kg.

Mechanistic studies

Assessment of membrane damage based on extracellular ATP levels

Previous work showed that some manganese(I) tricarbonyl complexes with antibacterial properties elicited membrane disruption, as evident from a detectable increase in the release of ATP.[38] As the Mn and Re cholate conjugates **9** and **10** presented in this paper feature the same $M(bpa)(CO)_3$ moiety, a similar approach was used to determine whether they also induce membrane disruption that could be involved in the mechanism of antibacterial action. Gram-negative (*A. baumannii* AB184) and Gram-positive (*S. aureus* SH1000) bacterial cultures were treated with **9** and **10** at sub-MIC concentrations and extracellular ATP levels were measured with a luciferin-based assay. However, in the case of AB184, the amount of ATP released after 120 min of incubation was even lower than that induced by DMSO applied as a control and in the case SH1000, the amount of extracellular ATP also did not correlate with incubation time and was generally low (Fig. 6). Thus, in contrast to the previously reported generation of Mn tricarbonyl compounds,[21] no ATP release was identified in response to treatment. Therefore, cellular membrane disruption does not appear to be involved in the mechanism of action of these complexes.

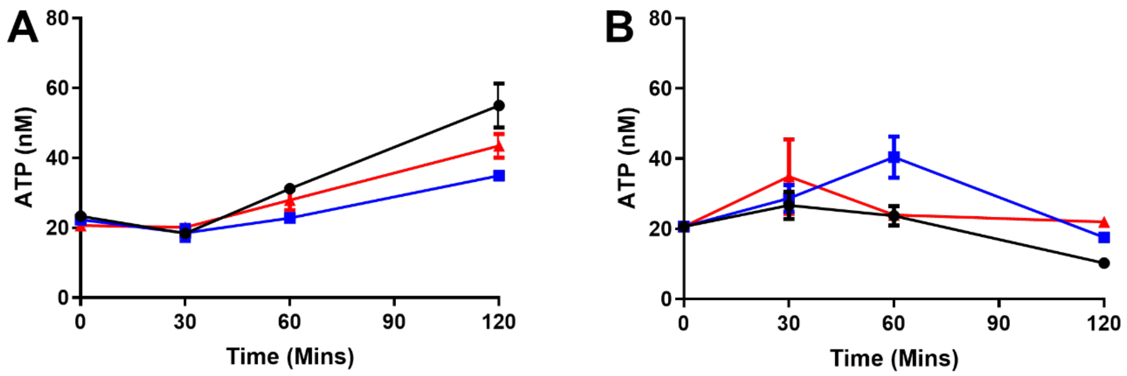

Figure 6. Changes in extracellular ATP released from AB184 (panel A) and SH1000 (panel B) cells were measured using recombinant luciferase and D-luciferin upon treatment with **9** (blue line) or **10** (red line) at half-MIC concentrations (32 μM for **9** and 16 μM for **10** with AB184; 2 μM for both compounds with SH1000). DMSO at 1% (black line) was used as a control. Data points represent the mean of three replicates and errors bars show the standard deviation. Standard curves were used to determine ATP content from measured luminescence.

Metal analysis by ICP-MS to study intracellular accumulation

ICP-MS analysis of the intracellular metal content of *E. coli* cells treated with [Mn(bqpa-κ^3N)(CO)$_3$]Br investigated previously highlighted a significant intracellular accumulation of manganese in response to treatment (Fig. S1).[21] Therefore, potential accumulation of cholate conjugates **9** and **10** was investigated with ICP-MS. The total metal content of Mn and Re in bacterial cells increased with incubation time following treatment with the respective cholate conjugate (Fig. 7A). Although this analysis method is unable to discriminate between uptake of the fully intact conjugate *vs*. part of the metal-binding moiety, the data suggests that at least part of the compounds enters the cells.

Therefore, several strains with knockouts in genes encoding for *E. coli* efflux pumps were initially tested against [Mn(bqpa-κ^3N)(CO)$_3$]Br serving as a control. OD_{595} values measured after 5 h of incubation for *acrB*$^-$, *acrD*$^-$, *and mdtF*$^-$ mutant strains exposed to the metal complex were significantly lower than those of wildtype *E. coli*, while only the *emr*$^-$ mutant showed significantly lower growth in the untreated samples compared to the wildtype, indicating that knock out of these pumps renders *E. coli* more sensitive to the manganese compound (Fig. S2A). This effect was apparent in the presence and absence of UV light exposure for the strains with mutations in the AcrB and AcrD subunits of multidrug efflux pumps known to export a wide range of antimicrobial compounds knocked out (Fig. S2C+D). RT-PCR also showed that *E. coli* increased expression of these genes in response to metal complex treatment (Fig. S2B). These data reinforce the idea that the compound enters cells and exerts intracellular antibacterial activity, with efflux required to attenuate the effect.

This increased sensitivity of efflux knockout mutants is also observed for **9** and **10** (Fig. 7B+C), which is in line with the ICP-MS data suggesting that the complexes act on an intracellular target. An *E. coli mntP* mutant with a knockout in a manganese exporter also showed an increased sensitivity to **9**, although this effect was apparent only when UV light activation was used to release the CO ligands and not with an intact Mn(CO)$_3$ moiety (Fig. 7C). The *mntP*$^-$ mutant did not show increased sensitivity to the rhenium analogue **10** with or without UV photoactivation. Again, this matches the results obtained for previously studied [Mn(bqpa-κ^3N)(CO)$_3$]Br. The *mntP* mutant strain of *E. coli* is more sensitive to the compound than the wildtype, while knockout of the regulator that controls expression of *mntP* and *mntH* ,which are involved in Mn uptake, increased the sensitivity to the compound to smaller degree. Furthermore, mutation of *mntH* had no effect on sensitivity. Expression of *mntP* (Mn efflux) increased and expression of *mntH* (Mn uptake) decreased in response to treatment with

[Mn(bqpa-κ^3*N*)$(CO)_3$]Br (Fig. S3). Expression of these genes is controlled by the MntR regulator that is located in the cytoplasm, further reinforcing the ICP data indicating increased intracellular Mn levels.[39] However, the molecular mechanism by which the Mn compound interacts with the regulator is currently unknown. Both direct binding as well as indirect modulation of intracellular Mn levels might lead to the effects observed.

In summary, the intact compounds, or at least some metal-containing fragment of them, accumulate inside the cell. The increased sensitivity of *E. coli* strains with a perturbed efflux due to gene knockout indicate that the compounds have an intracellular mechanism of action. AcrB and AcrD may not be responsible for, and capable of, carrying the compounds out of the cells, as the increased sensitivity may also be a result of alternative effects caused by the knockout of the genes encoding these efflux pump subunits.

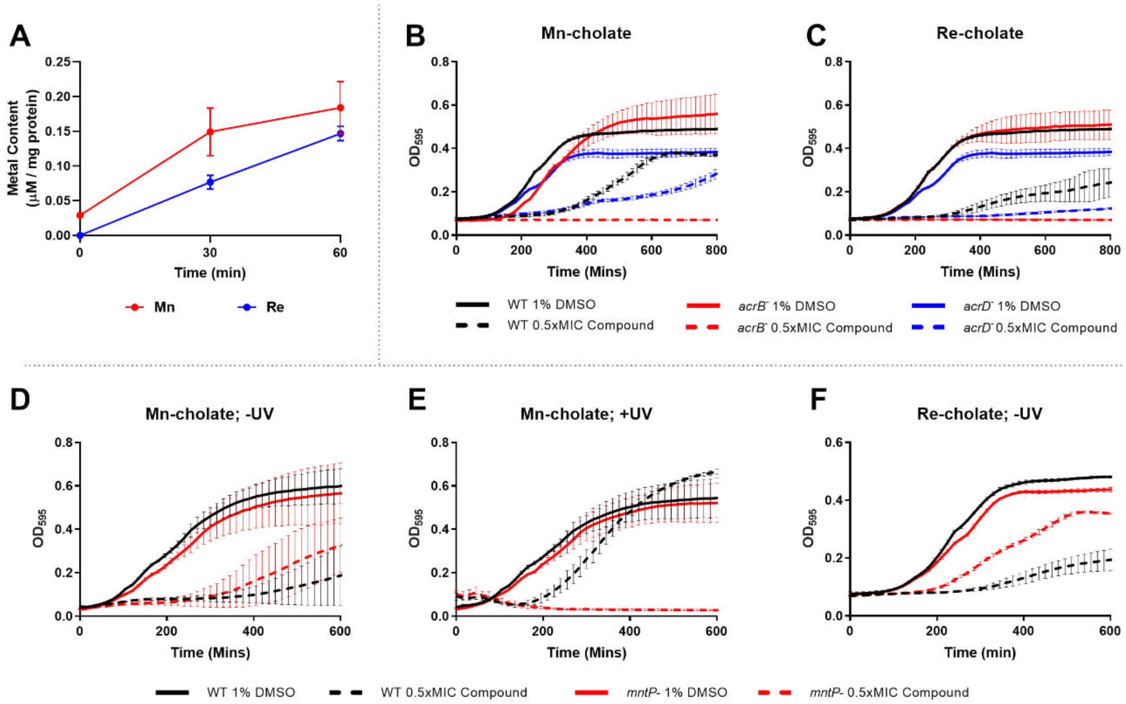

Figure 7. A) ICP-MS analysis of change in intracellular Mn and Re in *E. coli* cells treated with **9** and **10**. The level of rhenium at $t = 0$ was below the detection limit and thus is given as 0 for data display purposes only. B+C) Growth curves of *E. coli* mutants with the transporter genes *acrB* and *acrD* knocked out upon exposure to **9** (B) and **10** (C) in the absence of UV activation. D–F) Growth curves of *mntP*$^-$ *E. coli* relative to wildtype in response to **9** without (D) and with (E) UV photoactivation as well as **10** kept in the dark (F). All data points are the mean of three biological replicates with errors bars representing standard deviation.

Response of stress-sensitive mutants

In order to investigate the role of the cholate moiety, the sensitivity of *E. coli* single knockout mutants (from the Keio collection) with mutations in genes linked to bile salt and oxidative stress response (*dinF*, *yiaH*, *yciM*, *sodA*, *katE, soxS*) were tested against manganese complex **9**.[40-43] However, with the exception of YciM, no increased sensitivity compared to wildtype *E. coli* was observed (Fig. 8). Only mutation of the *yciM* gene led to a significant reduction in bacterial growth in the presence of the metal complex, but this effect is fairly ubiquitous with antimicrobials.[44] Overall, the antibacterial activity of compound **9** does not appear to be directly linked to either the presence of the cholate moiety or metal-induced stress from oxidation products of the $Mn(CO)_3$ group.[45, 46]

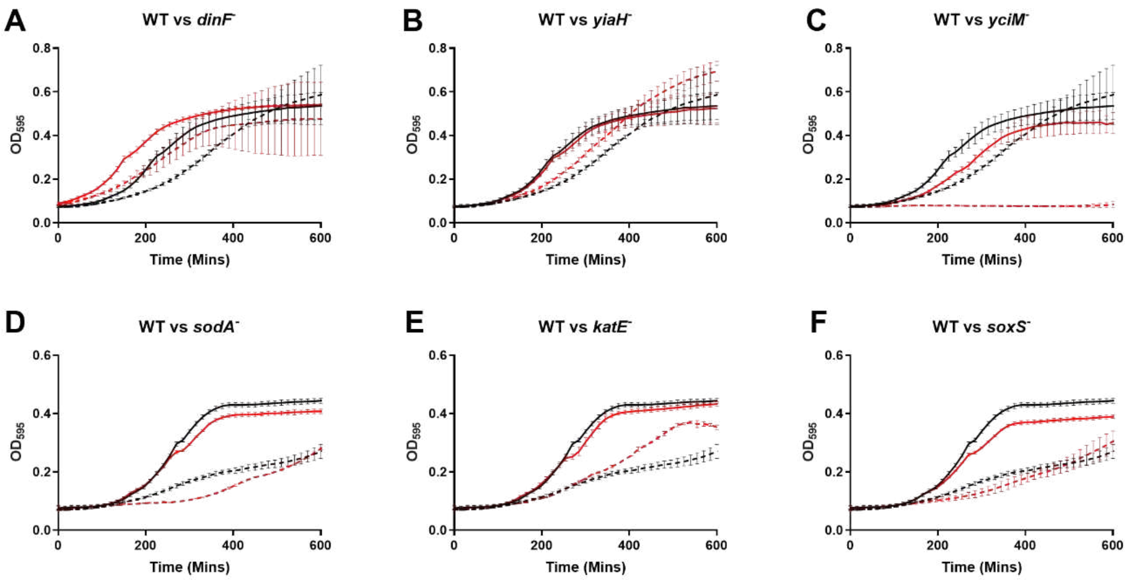

Figure 8. Growth curves of *E. coli* single-knockout strains from the Keio collection (red lines) compared to wild type BW25113 (black lines) in the presence of 1% DMSO (solid lines) or 400 μM $[Mn(bpen^{cholamide})(CO)_3]Br$ **9** (dashed lines). Points represent the mean OD_{595} of three replicates, and errors bars represent the standard deviation.

Conclusion

A bis(2-pyridylmethyl)amine (bpa) ligand was conjugated to a cholic acid carrier molecule in a simple DCC/NHS-mediated amide coupling on a gram scale. Reaction with manganese(I) or rhenium(I) pentacarbonyl bromide gave rise to $[M(bpen^{cholamide})(CO)_3]Br$ with M = Mn, Re in good yield and purity. The antibacterial activity of these bioconjugates was then explored on different bacterial strains with a special focus on methicillin-susceptible (MSSA) *vs.* methicillin-resistant (MRSA) *S. aureus* and compared to other bpa-type complexes. The two title compounds are potent antibacterial agents for the inhibition of MRSA/MSSA growth *in vitro* with MIC values in the very low micromolar range (2–4 μM). No significant difference in potency was observed for the Mn *vs*. Re complexes. While activity of the rhenium compound was not modulated by photoactivation, UV illumination of the manganese complex lead to some decrease in activity. Taken together these results strongly indicate that the compounds do not act as CO-releasing molecules (CORMs) but rather involve some other mode of activity. In the *Galleria mellonella* larvae model, both compounds were non-toxic at up to 100× MIC values, which corresponds to more than 200–300 μM. The manganese compound significantly increased the survival of larvae infected with MSSA and MRSA, with 88% survival in the treated *vs*. 46% survival in the non-treated control group. Detailed mechanistic studies were carried out on *E. coli* strains deficient in genes encoding drug efflux pumps as well as manganese uptake regulator proteins. Combined with ICP-MS measurements of metal uptake in bacterial cells and ATP release measurements, these results indicate that both the Mn and Re cholamide complexes are efficiently internalized by *E. coli* cells, do not interfere with membrane integrity, and show increased activity in efflux knockout mutants. Taken together, this strongly point to an intracellular mode of action that is not triggered by CO released from the metal complexes but rather involves the complete Mn or Re conjugate, or at least a significant part of it. As single knockout mutants defective in genes related to bile salt and oxidative stress response such as *dinF*, *yiaH*, *sodA*, *katE, soxS* did not show increased sensitivity relative to the wildtype, neither the cholic acid moiety nor the metal-carbonyl fragment alone appear to be responsible for the biological activity observed and the search for the primary intracellular target continues. Nevertheless, the facile synthesis on a scale of several 100 mg, absence of toxicity in *G. mellonella* at several hundred micromole per liter, and very low micromolar antibacterial activity in MSSA/MRSA demonstrate that these $Mn(bpa)(CO)_3$ and $Re(bpa)(CO)_3$ cholamide conjugates are interesting candidates for further metalloantibacterial drug development.

Experimental section

General remarks. All synthetic procedures were performed under anhydrous dinitrogen using standard Schlenk and vacuum-line techniques. NMR spectra were recorded on Bruker Avance 300 (^{1}H: 300.18 MHz, ^{13}C: 75.48 MHz)] and Bruker Avance 500 spectrometers (^{1}H: 500.13 MHz, ^{13}C: 125.75 MHz) with chemical shifts δ reported in ppm. The residual signal of the solvent was used for referencing.[47] Signal multiplicities are reported as singlet (s), doublet (d), doublet-of-a-doublet (dd), doublet-of-a-doublet-of-a-doublt (ddd), triplet (t), doublet-of-a-triplet (dt), triplet-of-a-doublet (td), quartet (q) or multiplet (m). Coupling constants *J* are reported in Hz. IR spectra were collected on a Nicolet 380 FT IR spectrometer with a smart iFTR accessory on pure solid samples. Signal intensities are reported as very strong (vs), strong (s), medium (m), weak (w), or broad (br). ESI mass spectra were recorded on a Thermo Fisher Exactive Plus Orbitrap mass spectrometer at a solvent flow rate of 10 µL/min. The CHN analysis was done with an Elementar Vario MicroCube instrument. All other chemicals were obtained from commerical sources and used as received.

Synthesis of *N*-(2-(bis(pyridin-2-ylmethyl)amino)ethyl)cholamide (bpen$^{\mathbf{cholamide}}$) (6). Cholic acid (1.68 g, 4.11 mmol), *N*-hydroxysuccinimide (0.52 g, 4.52 mmol) und dicyclohexylcarbodiimide (0.93 g, 4.51 mmol) were dissolved in tetrahydrofuran (30 mL) and stirred for 24 h at room temperature. The resulting colourless precipitate was filtered off, washed with tetrahydrofuran (10 mL), and the solid material discarded. To the colourless solution was slowly added *N*,*N*-bis(pyridin-2-ylmethyl)ethan-1,2-diamine (1.00 g, 4.13 mmol) and *N*,*N*-diisopropylethylamine (1.54 mL, 1.17 g, 9.05 mmol). The resulting pale yellow solution was stirred at room temperature for 24 h. Then, the solvent was removed under vacuum and the residue dissolved in dichlormethane (50 mL). After washing with water (100 mL), concentrated aqueous ammonium chloride (50 mL), saturated sodium hydrogen carbonate (50 mL), and brine (3 x 50 mL), the yellow organic phase was dried over sodium sulfate and then the solvent removed under vacuum. The resulting pale yellow solid was purified by column chromatography on silica with a mixture of dichlormethan and methanol (5:1 v/v) as the eluent to obtain the product (R_f = 0.45) as a colourless powder. Yield: 71% (1.84 g, 2.91 mmol). **IR** (ATR): $\tilde{\boldsymbol{\nu}}$ = 3222 (m), 2933 (m), 2862 (w), 1633 (s), 1570 (m), 764 (s) cm^{-1}; **^{1}H NMR** (500.13 MHz, DMSO-d_6): δ = 8.47 (ddd, 2H, $^3J_{\mathrm{H6,H5}}$ = 4.9 Hz, $^4J_{\mathrm{H6,H4}}$ = 1.8 Hz, $^5J_{\mathrm{H6,H3}}$ = 0.9 Hz, py-H6), 7.77 (t, 1H, ^3J = 5.8 Hz, CON*H*), 7.74 (dt, 2H, $^3J_{\mathrm{H4,H5/H3}}$ = 7.7 Hz, $^4J_{\mathrm{H4,H6}}$ = 1.8 Hz, py-H4), 7.53 (d, 2H, $^3J_{\mathrm{H3,H4}}$ = 7.8 Hz, py-H3), 7.24 (ddd, 2H, $^3J_{\mathrm{H5,H4}}$ = 7.5 Hz, $^3J_{\mathrm{H5,H6}}$ = 4.9 Hz, $^4J_{\mathrm{H5,H3}}$ = 1.2 Hz, py-H5), 4.32 (d, 1H, $^3J_{\mathrm{OH,CH}}$ = 4.4 Hz, cholic acid-C3-O*H*), 4.10 (d, 1H, $^{3}J_{\mathrm{OH,CH}}$ = 3.6 Hz, cholic acid-C12-O*H*), 4.01 (d, 1H, $^{3}J_{\mathrm{OH,CH}}$ = 3.5 Hz, cholic acid-C7-O*H*), 3.78 (m, 1H, cholic acid-H12), 3.76 (s, 4H, py-C*H*$_2$), 3.61 (m, 1H, cholic acid-H7), 3.19 (m, 3H, C*H*$_2$NHCO+cholic acid-H3), 2.54 (t, 2H, ^{3}J = 6.6 Hz, (py-CH$_2$)$_2$NC*H*$_2$), 2.33 – 0.73 (m, 30H, cholic acid-CH$_3$/CH$_2$/CH), 0.56 (s, 3H, cholic acid-C18-C*H*$_3$) ppm; **^{13}C NMR** (125.76 MHz, DMSO-*d*$_6$): δ = 172.43 (*C*ONH), 159.34 (py-C2), 148.68 (py-*C*6), 136.41 (py-*C*4), 122.59 (py-*C*3), 122.08 (py-*C*5), 71.00 (cholic acid-*C*12), 70.43 (cholic acid-*C*3), 66.24 (cholic acid-*C*7), 59.59 (py-*C*H$_2$), 53.17 ((py-CH$_2$)$_2$N*C*H$_2$), 46.09 (cholic acid-*C*17), 45.71 (cholic acid-*C*13), 41.52 (cholic acid-*C*5), 41.38 (cholic acid-*C*14), 40.04 (cholic acid-*C*4, overlapping with solvent peak), 39.95 (cholic acid-*C*8, overlapping with solvent peak), 36.62 (*C*H$_2$NHCO), 35.31 (cholic acid-*C*1), 35.15 (cholic acid-*C*20), 34.89 (cholic acid-*C*6), 34.38 (cholic acid-*C*10), 32.53 (cholic acid-*C*23), 31.71 (cholic acid-*C*22), 30.40 (cholic acid-*C*2), 28.57 (cholic acid-*C*11), 27.29 (cholic acid-*C*16), 26.22 (cholic acid-*C*9), 22.79 (cholic acid-*C*15), 22.63 (cholic acid-*C*19), 17.12 (cholic acid-*C*21), 12.33 (cholic acid-*C*18) ppm; **MS** (ESI$^+$, CH$_3$OH): *m*/*z* = 633.4343 [M+H]$^+$, 655.4163 [M+Na]$^+$,1287.8439 [2M+Na]$^+$; **Elemental analysis** (%) calcd. for $C_{38}H_{56}N_4O_4 \cdot H_2O$: C 70.12, H 8.98, N 8.61; found (%): C 69.67, H 8.97, N 8.79.

Synthesis of [Mn(bpen$^{\mathbf{cholamide}}$-κ^3*N*)(CO)$_3$]Br (9). Manganese pentacarbonyl bromide (261 mg, 0.95 mmol) and *N*-(2-(bis(pyridin-2-ylmethyl)amino)ethyl)cholamide (600 mg, 0.95 mmol) were dissolved under argon in anhydrous degassed dichlormethane (50 mL) and then heated to reflux under protection from light for 3 h. Then, the solvent was removed under vacuum and the solid residue washed with diethyl ether (3 x 30 ml). After drying under vacuum, the product was obtained as a yellow powder. Yield: 76% (614 mg, 0.72 mmol). **IR** (ATR): $\tilde{\nu}$ = 3270 (br), 2937 (w), 2023 (vs), 1914 (vs), 1657 (w), 1611 (w), 1536 (w), 1444 (w), 769 (w) cm^{-1}; **^{1}H NMR** (500.13 MHz, DMSO-*d*$_6$): δ = 8.87 (d, 2H, $^{3}J_{\mathrm{H6,H5}}$ = 5.3 Hz, py-H6), 8.10 (t, 1H, ^{3}J = 5.0 Hz, CON*H*), 7.91 (t, 2H, $^{3}J_{\mathrm{H4,H5/H3}}$ = 7.6 Hz, py-*H*4), 7.43 (m, 4H, py-*H*3, py-*H*5), 4.88 (d, 2H, ^{2}J = 16.7 Hz, py-C*H*$_2$), 4.71 (d, 2H, ^{2}J = 17.0 Hz, py-C*H*$_2$), 4.32 (d, 1H, $^{3}J_{\mathrm{OH,CH}}$ = 3.8 Hz, cholic acid-C3-O*H*), 4.10 (d, 1H, $^{3}J_{\mathrm{OH,CH}}$ = 3.3 Hz, cholic acid-C12-O*H*), 4.00 (d, 1H, $^{3}J_{\mathrm{OH,CH}}$ = 3.1 Hz, cholic acid-C7-O*H*), 3.78 (m, 3H, (py-CH$_2$)$_2$NC*H*$_2$+cholic acid-H12), 3.61 (m, 3H, C*H*$_2$NHCO+cholic acid-H7), 3.18 (m, 1H, cholic acid-H12), 2.31 – 0.71 (m, 30H, cholic acid-C*H*$_3$/C*H*$_2$/C*H*), 0.58 (s, 3H, cholic acid-C18-C*H*$_3$) ppm; **^{13}C NMR** (125.76 MHz, DMSO-*d*$_6$): δ = 218.90 (*C*O), 218.35 (*C*O), 173.15 (*C*ONH), 160.26 (py-*C*2), 152.09 (py-*C*6), 139.60 (py-*C*4), 125.37 (py-*C*3), 122.50 (py-*C*5), 70.96 (cholic acid-*C*12), 70.37 (cholic acid-*C*3), 66.85 ((py-CH$_2$)$_2$N*C*H$_2$), 66.27 (py-*C*H$_2$), 66.19 (cholic acid -*C*7), 46.11 (cholic acid-*C*17), 45.68 (cholic acid-*C*13), 41.46 (cholic acid-*C*5), 41.37 (cholic acid-*C*14), 40.02 (cholic acid-*C*4, overlapping with solvent peak), 39.94 (cholic acid-*C*8, overlapping with solvent peak), 35.26 (cholic acid-*C*1), 35.12 (cholic acid-*C*20), 34.86 (cholic acid-*C*6), 34.40 (CH_2NHCO), 34.34 (cholic acid-*C*10), 32.46 (cholic acid-*C*23), 31.61 (cholic acid-*C*22), 30.36 (cholic acid-*C*2), 28.53 (cholic acid-*C*11), 27.33 (cholic acid-*C*16), 26.19 (cholic acid-*C*9), 22.76 (cholic acid-*C*15), 22.60 (cholic acid-*C*19), 17.07 (cholic acid-*C*21), 12.25 (cholic acid-*C*18) ppm; **MS** (ESI^+, CH_3OH): *m*/*z* = 771.3471 $[M\text{-}Br]^+$; **Elemental analysis** (%) calcd. for $C_{41}H_{56}BrMnN_4O_7 \cdot 2\ H_2O$: C 55.47, H 6.81, N 6.31; found (%): C 55.67, H 6.77, N 6.68.

Synthesis of [Re(bpen$^{\text{cholamide}}$-κ^3*N*)(CO)$_3$]Br (10). Rhenium pentacarbonyl bromide (320 mg, 0.79 mmol) and *N*-(2-(bis(pyridin-2-ylmethyl)-amino)ethyl)cholamide (500 mg, 0.79 mmol) were dissolved under argon in anhydrous degassed toluene (20 mL) and then heated to reflux for 3 h. After removal of the solvent under vacuum, the residue was dissolved in a mixture of dichlormethane, acetone, and ethanol (10:10:1 v/v/v, 52.5 mL) and then precipitated by addition of diethyl ether (100 mL). The resulting colourless solid was collected by filtration and washed with diethyl ether (20 mL). After drying under vaccum overnight, the product was obtained as a colourless solid. Yield: 41% (318 mg, 0.32 mmol). **IR** (ATR): $\tilde{\nu}$ = 3383 (br), 2930 (m), 2028 (vs), 1902 (vs), 1657 (w), 1611 (w), 1535 (w), 1441 (w), 767 (w) cm^{-1}; **^{1}H NMR** (500.13 MHz, DMSO-d_6): δ = 8.80 (d, 2H, $^3J_{H6,H5}$ = 5.3 Hz, py-H6), 8.10 (t, 1H, ^3J = 5.2 Hz, CON*H*), 7.99 (dt, 2H, $^3J_{H4,H5/H3}$ = 8.3 Hz, $^4J_{H4,H6}$ = 1.4 Hz, py-*H*4), 7.55 (d, 2H, $^3J_{H3,H4}$ = 7.8 Hz, py-*H*3), 7.40 (t, 2H, $^3J_{H5,H4/H6}$ = 6.5 Hz, py-*H*5), 5.04 (d, 2H, ^2J = 17.1 Hz, py-CH_2), 4.95 (d, 2H, ^2J = 16.5 Hz, py-CH_2), 4.32 (d, 1H, $^3J_{OH,CH}$ = 4.3 Hz, cholic acid-C3-O*H*), 4.10 (d, 1H, $^3J_{OH,CH}$ = 3.3 Hz, cholic acid-C12-O*H*), 4.00 (d, 1H, $^3J_{OH,CH}$ = 3.1 Hz, cholic acid-C7-O*H*), 3.83 (t, 2H, ^3J = 7.0 Hz, (py-CH_2)$_2$NCH_2), 3.78 (m, 1H, cholic acid-H12), 3.60 (m, 3H, CH_2NHCO+cholic acid-H7), 3.19 (m, 1H, cholic acid-H3), 2.28 – 0.74 (m, 30H, cholic acid-CH_3/CH_2/C*H*), 0.58 (s, 3H, cholic acid-C18-CH_3) ppm; **^{13}C NMR** (125.76 MHz, DMSO-d_6): δ = 196.38 (*C*O), 195.16 (*C*O), 173.19 (*C*ONH), 160.52 (py-*C*2), 151.78 (py-*C*6), 140.65 (py-*C*4), 125.76 (py-*C*3), 123.40 (py-*C*5), 70.99 (cholic acid-*C*12), 70.40 (cholic acid-*C*3), 67.87 ((py-CH_2)$_2$NCH_2), 66.99 (py-CH_2), 66.22 (cholic acid-*C*7), 46.12 (cholic acid-*C*17), 45.71 (cholic acid-*C*13), 41.49 (cholic acid-*C*5), 41.40 (cholic acid-*C*14), 40.03 (cholic acid-*C*4, overlapping with solvent peak), 39.94 (cholic acid-*C*8, overlapping with solvent peak), 35.29 (cholic acid-*C*1), 35.15 (cholic acid-*C*20), 34.89 (cholic acid-*C*6/*C*10, two overlapping signals), 34.37 (CH_2NHCO), 32.46 (cholic acid-*C*23), 31.63 (cholic acid-*C*22), 30.39 (cholic acid-*C*2), 28.56 (cholic acid-*C*11), 27.36 (cholic acid-*C*16), 26.22 (cholic acid-*C*9), 22.79 (cholic acid-*C*15), 22.63 (cholic acid-*C*19), 17.10 (cholic acid-*C*21), 12.30 (cholic acid-*C*18) ppm; **MS** (ESI^+, CH_3OH): *m/z* = 903.3671 $[M-Br]^+$; **Elemental analysis** (%) calcd. for $C_{41}H_{56}BrN_4O_7Re \cdot 4\ H_2O$: C 46.67, H 6.11, N 5.31; found (%): C 45.86, H 5.99, N 5.60.

Microbiological methods

Chemicals, media, bacterial isolates, and larvae. Luria broth base, Mueller-Hinton 2 (MH2) cation-adjusted broth and cell culture media/supplements were purchased from Sigma-Aldrich (Dorset, UK). MRSA strain NCTC 12493 and MSSA strain NCTC 12981 were purchased from Pro-Lab Diagnostics (Wirral, UK). MRSA strain USA300 and MSSA strain SH1000 were from the Network for Antimicrobial Resistance in *S. aureus* (NARSA) collection (Eurofins, VA). EC958, a multidrug-resistant clinical isolate of uropathogenic *E. coli* ST131 was obtained from ___ [Source still missing → Calum, Robert???] *E. coli* knockout mutant strains utilised were from the Keio collection, and the parent strain BW25113 was used as the wildtype for comparison. *Acinetobacter baumannii* isolates AB184 and AB210 were provided by the Royal London Hospital (Whitechapel, UK). Isolates were stored on cryobeads at -80 °C until required. Antibiotic susceptibility profiles were determined prior to any further testing. All *in vivo* assays were performed using the *Galleria mellonella* TruLarv model (Biosystems Technology, Exeter, UK). Experimental studies using *G. mellonella* are not subject to any regulation under the Animals Scientific Procedures Act (ASPA) 1986.

The minimum inhibitory concentration (MIC) of **9** and **10** were determined *via* microdilution assays in MH2 broth versus MRSA and MSSA. Microtitre plates were incubated at 37 °C aerobically for 18–20 h, after which MICs were recorded. Kill kinetics of both compounds were also determined in MH2 broth versus MRSA and MSSA strains over 24 h. In brief, a 1/1000 dilution of a 18–20 h bacterial culture, with an approximate CFU/mL of 10^6, was used as the starting inoculum for all strains. To individual cultures, antimicrobials were added at x1 MIC. Cultures were incubated at 37 °C on an orbital shaker (225 rpm) for 24 h. At fixed time intervals of 0, 2, 4, 6, and 24 h post inoculation, 100 µL samples were collected, serially diluted, and plated onto MH2 agar. Viable counts were determined after incubation aerobically at 37 °C for 18–20 h. Growth curves of bacterial strains were determined using a Tecan Sunrise microplate reader using 96-well microtiter plates. Overnight cultures were diluted 1/100 into fresh MH2 broth and grown aerobically in volumes of 100 µL at 37 °C. UV activation of the manganese compound was performed as described previously.[30]

The toxicity of **9** and **10** was determined in greater wax moth (*Galleria mellonella*) larvae at concentrations of between 10 and 100 times that required for bacterial inhibition. *Via* a left proleg, 10 µL injections of complex **9** at 10× and 100× MIC for MSSA NCTC 12981 (31 and 310 µM in 5% DMSO, respectively) and complex **10** at 10× and 100× MIC for MSSA NCTC 12981 (34 and 340 µM in 5% DMSO) were administered. Phosphate buffered saline (PBS) and MSSA strain NCTC 12981 were used as a negative and positive controls, respectively. Larvae were incubated at 37 °C for 96 h aerobically. At 24 h time points, larvae were scored for survival (live/dead), where death was classified as an absence of movement in response to stimulation. The *in vivo* efficacy of **9** *vs*. MSSA and MRSA strains was determined in the *G. mellonella* model of infection as previously described. In brief, overnight cultures (18–20 h) of each strain were washed with PBS and serially diluted. Then, a 10 µL injection *via* a left proleg was administered to 16 larvae per group, containing an inoculum that would result in staggered killing over 96 h. After 15 min, larvae were then injected, *via* a right proleg, with a concentration of **9** dissolved in 5% DMSO, equivalent to 10× of the concentration required for bacterial inhibition (0.8–1.07 mg/kg). Larvae were incubated aerobically at 37 °C for 96 h. Every 24 h, larvae were scored for survival as described above. The Mantel-Cox Log rank test was performed to test for significant differences in larval survival.

Bioluminescence-based ATP release assays

The level of extracellular ATP in bacterial cultures following treatment with compounds was determined as previously described using the Molecular Probes ATP Determination Kit (Invitrogen) and a Lumat3 LB 9508 Luminometer (Berthold Technologies).[21]

Metal content determination by ICP-MS

Intracellular metal content was determined by inductively coupled plasma mass spectrometry (ICP-MS). Bacterial cultures were grown to mid-log phase and harvested via centrifugation (10,000 × g at 10 °C for 20 min). Pellets were washed three times in wash buffer (10 mM HEPES, 0.5 M sorbitol, 100 µM EDTA, pH 7.5) and then washed once in the buffer without the EDTA. Washed pellets were resuspended in 65% nitric acid and left at room temperature for a minimum of 48 h. The relative abundance of selected metals was determined using ICP-MS on a Agilent 4500 instrument in the Department of Chemistry, The University of Sheffield. The protein concentration of intact cells from each sample analysed by ICP-MS was determined simultaneously using the Lowry method.

RNA extraction and gene expression analysis by qRT-PCR

RNA extraction and qRT-PCR were conducted as previously described.[48] Briefly, RNA was extracted from mid-log phase cells with and without treatment with [Mn(bqpa-κ^3*N*)$(CO)_3$]Br using the TRIzol Max Bacterial RNA Isolation Kit (Thermo Fisher Scientific) with additional DNase treatment using a Turbo DNA-free kit (Ambion). Reverse transcription-quantitative PCR (qRT-PCR) was performed using a SensiFAST SYBR Lo-ROX one-step kit (Bioline) in 96-well optical reaction plates, with each reaction performed in technical triplicate. A standard curve for each pair of primers was produced using *E. coli* genomic DNA, and gene expression was calculated relative to the reference gene *gyrA*. PCR amplification was performed using a Stratagene MX3005p thermal cycler (Agilent) and relative gene expression levels were calculated using the comparative method described in the user bulletin 2 of the ABI Prism 700 sequence detection system. Primer pairs used were designed using Primer3web (Version 4.1):
acrB: 5'-TAATTTCTTTATCGATCGCC-3' and 5'-GTCACTGTTAGAGGACATGTA-3'
acrD: 5'-TCTTTATTGATCGCCCCATT-3' and 5'-TATCGAGGCCGGTCATATTT-3'
mntP: 5'-ATCACTGCTACTGTTCTTCTTGC-3' and 5'-TAACATGCCCATTCCCCAGC-3'
mntH: 5'-TAGCAGCGGACGGGCG-3' and 5'-CAAACGACAACCCACAGTAGC-3'
gyrA: 5'-GGTACACCGTCGCGTACTTT-3' and 5'-TACCGATTACGTCACCAACG-3'

Acknowledgements

This work was supported by the Deutsche Forschungsgemeinschaft (DFG) with grant no. SCHA962/9-1 to U.S. and the Biotechnology and Biological Sciences Research Council (BBSRC) with grant no. BB/M022579/1 to R.K.P.

References

1 M. Stadler and P. Dersch, eds., *How to overcome the antibiotic crisis: Facts, challenges, technologies, and future perspectives*, Springer, Cham, 2016.

2 S. T. Cole, *Phil. Trans. Royal. Soc. B*, 2014, **369**, 2013043.

3 M. Lakemeyer, W. Zhao, F. A. Mandl, P. Hammann and S. A. Sieber, *Angew. Chem. Int. Ed.*, 2018, **57**, 14440.

4 F. Li, J. G. Collins and F. R. Keene, *Chem. Soc. Rev.*, 2015, **44**, 2529.

5 A. Frei, J. Zuegg, A. G. Elliott, M. Baker, S. Bräse, C. Brown, F. Chen, C. G. Dowson, G. Dujardin, N. Jung, A. P. King, A. M. Mansour, M. Massi, J. Moat, H. A. Mohammad, A. K. Renfrew, P. J. Rutledge, P. J. Sadler, M. H. Todd, C. Willans, E., J. J. Wilson, M. A. Cooper and M. A. T. Balskovich, *Chem. Sci.*, 2020, **11**, 2627.

6 P. V. Simpson, C. Nagel, H. Bruhn and U. Schatzschneider, *Organometallics*, 2015, **34**, 3809.

7 B. Albada and N. Metzler-Nolte, *Acc. Chem. Res.*, 2017, **50**, 2510.

8 P. D. Savage and C. Li, *Expert Opin. Invest. Drugs*, 2000, **9** 263.

9 X.-Z. Lai, Y. Feng, J. Pollard, J. N. Chin, M. J. Rybak, R. Bucki, R. F. Epand, R. M. Epand and P. B. Savage, *Acc. Chem. Res.*, 2008, **41**, 1233.

10 M. Blanchet and J. M. Brunel, *Curr. Med. Chem.*, 2018, **25**, 3613.

11 R. Sharma, A. Long and J. F. Gilmer, *Curr. Med. Chem.*, 2011, **18**, 4029.

12 R. A. S. Randazzo, R. Bucki, P. A. Janmey and S. L. Diamond, *Bioorg. Med. Chem.*, 2009, **17**, 3257.

13 L. Huang, H. Zhu, G. Liu, J. Xu and Y.-M. Shen, *Chin. J. Org. Chem.*, 2009, **29**, 396.

14 C. Faustino, C. Serafim, P. Rijo and C. Pinto Reis, *Expert Opin. Drug Deliv.*, 2016, **13**, 1133.

15 F. Le Bideau and S. Dagorne, *Chem. Rev.*, 2013, **113**, 7793.

16 L. Huang, H. Zhu, X. Xu, C. Zhang and Y.-M. Shen, *J. Organomet. Chem.*, 2009, **694**, 3247.

17 S. Neyt, M. Vliegen, B. Berreet, S. De Lombaerde, K. Braeckman, C. Vanhove, M. T. Huisman, C. Dumolyn, K. Kersemans, F. Hulpia, S. Van Calenbergh, G. Mannens and F. De Vos, *Nucl. Med. Biol.*, 2016, **43**, 642.

18 M. Assfalg, E. Gianolio, S. Zanzoni, S. Tomaselli, V. Lo Russo, C. Cabella, L. Ragona, S. Aime and H. Molinari, *J. Med. Chem.*, 2007, **50**, 5257.

19 L. Huang, Y. Sun, H. Zhu, J. Xu and Y.-M. Shen, *Steroids*, 2009, **74**, 701.

20 C. Nagel, S. McLean, R. K. Poole, H. Braunschweig, T. Kramer and U. Schatzschneider, *Dalton Trans.*, 2014, **43**, 9986.

21 P. Güntzel, C. Nagel, J. Weigelt, J. W. Betts, C. A. Pattrick, H. M. Southam, R. M. La Ragione, R. K. Poole and U. Schatzschneider, *Metallomics*, 2019, **11**, 2033.

22 J. Niesel, A. Pinto, H. W. Peindy N'Dongo, K. Merz, I. Ott, R. Gust and U. Schatzschneider, *Chem. Commun.*, 2008, 1798.

23 H. Pfeiffer, A. Rojas, J. Niesel and U. Schatzschneider, *Dalton Trans.*, 2009, 4292.

24 G. Dördelmann, H. Pfeiffer, A. Birkner and U. Schatzschneider, *Inorg. Chem.*, 2011, **50**, 4362.

25 G. Dördelmann, T. Meinhardt, T. Sowik, A. Krüger and U. Schatzschneider, *Chem. Commun.*, 2012, **48**, 11528.

26 S. Pai, M. Hafftlang, G. Atongo, C. Nagel, J. Niesel, S. Botov, H.-G. Schmalz, B. Yard and U. Schatzschneider, *Dalton Trans.*, 2014, **43**, 8664.

27 S. Pai, K. Radacki and U. Schatzschneider, *Eur. J. Inorg. Chem.*, 2014, 2886.

28 M. Tinajero-Trejo, N. Rana, C. Nagel, H. E. Jesse, T. W. Smith, L. K. Wareham, M. Hippler, U. Schatzschneider and R. K. Poole, *Antioxid. Redox Signal.*, 2016, **24**, 765.

29 J. Betts, C. Nagel, U. Schatzschneider, R. K. Poole and R. M. La Ragione, *PLOS ONE*, 2017, **12**, e0186359.

30 N. Rana, H. E. Jesse, M. Tinajero-Trejo, J. A. Butler, J. D. Tarlit, M. L. von und zur Mühlen, C. Nagel, U. Schatzschneider and R. K. Poole, *Microbiology*, 2017, **163**, 1466.

31 C. D. Incarvito, M. Lam, B. Rhatigan, A. L. Rheingold, C. J. Qin, A. L. Gavrilova and B. Bosnich, *Dalton Trans.*, 2001, 3478.

32 K. Kiyose, H. Kojima, Y. Urano and T. Nagano, *J. Am. Chem. Soc.*, 2006, **128**, 6548.

33 M. Vonlathen, C. M. Connelly, A. Deiters, A. Linden and N. S. Finney, *J. Org. Chem.*, 2014, **79**, 6054.

34 H.-J. Kallmayer and K.-H. Seyfang, *Arch. Pharm.*, 1980, **313**, 603.

35 Y.-H. Chiu and J. W. Canary, *Inorg. Chem.*, 2003, **42**, 5107.

36 U. Schatzschneider, *Eur. J. Inorg. Chem.*, 2010, 1451.

37 U. Schatzschneider, *Br. J. Pharmacol.*, 2015, **172**, 1638.

38 M. Yasir, D. Dutta and M. D. P. Willcox, *Sci. Rep.*, 2019, **9**, 7063.

39 J. E. Martin, L. S. Waters, G. Storz and J. A. Imlay, *PLOS Genet.*, 2015, **11**, e1004977.

40 J. Rodriguez-Beltran, A. Rodriguez-Rojas, J. R. Guelfo, A. Couce and J. Blazquez, *PLOS ONE*, 2012, **7**, e34791.

41 J. Kajimura, A. Rahman, J. Hsu, M. Evans, R., K. H. Gardner and P. D. Rick, *J. Bacteriol.*, 2006, **188**, 7542.

42 S. Mahalakshmi, M. R. Sunayana, L. SaiSree and M. Reddy, *Mol. Microbiol.*, 2014, **91**, 145.

43 M. E. Merritt and J. R. Donaldson, *J. Med. Microbiol.*, 2009, **58**, 1533.

44 A. Liu, L. Tran, E. Becket, K. Lee, L. Chinn, E. Park, K. Tran and J. H. Miller, *Antimicrob. Agents Chemother.*, 2010, **54**, 1393.

45 H.-M. Berends and P. Kurz, *Inorg. Chim. Acta*, 2012, **380**, 141.

46 U. Sachs, G. Schaper, D. Winkler, D. Kratzert and P. Kurz, *Dalton Trans.*, 2016, **45**, 17464.

47 G. R. Fulmer, A. J. M. Miller, N. H. Sherden, H. E. Gottlieb, A. Nudelman, B. M. Stoltz, J. E. Bercaw and K. I. Goldberg, *Organometallics*, 2010, **29**, 2176.

48 C. A. Pattrick, J. P. Webb, J. Green, R. R. Chaudhuri, M. O. Collins and D. J. Kelley, *mSystems*, 2019, **4**, e00163.